NASA TECHNICAL NOTE

NASA TN D-5211

NASA TN D-5211

ANALYSIS OF GOLD SPHERE TRANSMISSION EXPERIMENTS AT 24-keV NEUTRON ENERGY USING SPIN-DEPENDENT s-WAVE STATISTICS

by Thor T. Semler

Lewis Research Center
Cleveland, Ohio

NATIONAL AERONAUTICS AND SPACE ADMINISTRATION • WASHINGTON, D. C. • MAY 1969

NASA TN D-5211

ANALYSIS OF GOLD SPHERE TRANSMISSION EXPERIMENTS AT 24-keV NEUTRON ENERGY USING SPIN-DEPENDENT s-WAVE STATISTICS

By Thor T. Semler

Lewis Research Center
Cleveland, Ohio

NATIONAL AERONAUTICS AND SPACE ADMINISTRATION

For sale by the Clearinghouse for Federal Scientific and Technical Information
Springfield, Virginia 22151 – CFSTI price $3.00

ABSTRACT

The average capture cross section for gold $\bar{\sigma}_c$ at a neutron energy of 24 keV has been obtained by analysis of published sphere transmission experiments that use Sb-Be source neutrons. The analysis compares results using merged s-wave spin-state statistical data and separated spin-state statistical data. Values of $\bar{\sigma}_c$ of 725±30 mb are obtained using separated spin-state data and 660±30 mb using merged spin-state data. The value of 725±30 mb is in agreement with the larger of recent gold activation cross section measurements at 24 keV, which have a range of from 640±25 mb to 713±40 mb for the average capture cross section

ANALYSIS OF GOLD SPHERE TRANSMISSION EXPERIMENTS AT 24-keV NEUTRON ENERGY USING SPIN-DEPENDENT s-WAVE STATISTICS

by Thor T. Semler

Lewis Research Center

SUMMARY

A Monte Carlo analysis of spherical shell transmission experiments for gold at a neutron energy of 24 keV is presented. In the analysis, published spin-dependent neutron strength functions are used to generate s-wave cross sections.

A total of 10^6 cross sections are generated. A choice of the best sample of 10^4 cross sections, as determined by the Central Limit Theorem is made. These cross sections are used as input to the transmission program.

The potential cross section σ_{pot} is chosen as a parameter to conserve the independently measured value of the total cross section σ_{tot} for gold of 13.67 barns. For a given value of σ_{pot}, several values of the average p-wave capture cross section $\overline{\sigma_{c_p}}$ are introduced, and values of the neutron transmission are computed for each experimental shell. The value of $\overline{\sigma_{c_p}}$ compatible with the experimentally measured transmission is found by interpolation of several Monte Carlo solutions. This procedure is repeated for several values of σ_{pot}. The final value of $\overline{\sigma_{c_p}}$ is obtained as the value compatible with the measured transmission for a particular shell, and the total cross section since $\sigma_{tot} = \sigma_{pot} + \overline{\sigma_{s_s}} + \overline{\sigma_{c_s}} + \overline{\sigma_{c_p}}$ (where $\overline{\sigma_{s_s}}$ and $\overline{\sigma_{c_s}}$ are, respectively, the average s-wave scattering and capture cross sections).

Thus one obtains from the Monte Carlo analysis and the shell transmission experiments a set of cross sections which match the shell transmission and conserve the value of the total cross section.

A value of $\overline{\sigma_c}$ at 24 keV for gold of 725±30 millibarns is obtained using separated s-wave spin-state data compared with a value of 660±30 millibarns using merged s-wave spin-state data. This value is in agreement with the larger values of recent gold activation cross section measurements at 24 keV, which range from 640±25 to 713±40 millibarns for the average capture cross section

INTRODUCTION

Neutron capture cross section measurements in the keV energy region are of considerable interest to fields as diverse as cosmology and reactor design. Of particular interest are precise neutron capture cross sections for gold which could serve as a convenient secondary standard in the measurement of other isotopic capture cross sections. The status of the gold capture cross sections has been discussed recently by Cox (ref. 1) and by Poenitz (ref. 2). Attempts have been made to explain the discrepancies and to reconcile the various measurements in the keV region by Bogart (ref. 3) and by Poenitz, Kompe, and Menlove (ref. 4) who have discussed the persisting difficulties.

Most of the measurements below 200 keV rely on a normalization to activation cross sections at 30 keV or to sphere transmission results using antimony-beryllium (Sb-Be) source neutrons of nominally 24 keV. A summary of these cross sections for gold has been presented by Ryves et al. (ref. 5) who notes that recent activation cross sections amended to correspond to 24.8 keV vary from 713±40 millibarns of Harris et al. (ref. 6) to 679±70 millibarns of Poenitz (ref. 2) to 640±25 millibarns of Ryves et al. (ref. 5).

The shell transmission measurements provided values of 532±60 and 605±30 millibarns (refs. 7 and 8, see table I). However, the corrections for resonance self-protection that had been applied to the sphere transmission experiments (ref. 7) were found to be inadequate. A Monte Carlo interpretation of these experiments (reported in refs. 9 and 10) using merged spin s-wave statistics to generate cross sections at 24 keV, provided larger values of cross sections of 635±50 millibarns (ref. 7) and 660±50 millibarns (ref. 8).

TABLE I. - PREVIOUS ANALYSES OF GOLD-197

SPHERE TRANSMISSION EXPERIMENTS

Experiment	Data from -		
	Original source	Bogart and Semler (ref. 9)	This work
	Capture cross sections, σ_c, mb		
[a]Au I	532±60	620±50	710±31
[a]Au II	518±90	635±60	737±33
[b]Long counter	570±30	640±60	774±31

[a]Ref. 7.
[b]Ref. 8.

With the recent availability of separated spin-dependent s-wave statistics for gold (ref. 11), the Monte Carlo analysis of the sphere transmission experiments has been remade in an attempt to improve the precision of the average gold capture cross section at 24 keV.

SPHERE TRANSMISSION EXPERIMENT AND ANALYSIS

The experiments to be analyzed (refs. 7 and 8) used a monoenergetic Sb-Be neutron source inside of a spherical shell of the material whose cross section is to be measured. A flat-response neutron detector or water bath measures the number of neutrons emergent for the shell surrounding the source and the bare source. The observed values of transmission are corrected for finite source size and other effects, including the small group of higher energy neutrons emitted by the Sb-Be source. The corrected values of transmission are the ratios of the number of neutrons escaping the spherical shell of material to those emitted by a point source of 24 keV neutrons centrally located in the spherical shell of material.

From these values of transmission, a value for the average capture cross section can be obtained by an analysis due to Bethe et al. (refs. 12 to 14) which assumes cross sections to vary smoothly with neutron energy. Although the assumption of smoothly varying cross sections may be valid in the MeV energy region, at lower energies the assumption is questionable because of the significant peaking of individual resonances. The difficulties encountered when analysis of references 12 to 14 is applied to transmission experiments at 24 keV have been illustrated in reference 9.

The Monte Carlo analyses made herein follow the multiple scatterings of the neutrons in the material, and use directly the pointwise cross sections in the unresolved energy region generated by level statistics obtained from the resolved region.

MONTE CARLO TRANSMISSION CALCULATION

A Monte Carlo spherical transmission code is used to analyze the gold shell transmission experiments of Schmitt and Cook (ref. 7) and those of Belanova et al. (ref. 8). The Monte Carlo code assumes a point isotropic source of neutrons located at the center of a hollow spherical shell of material. The collision trajectories are followed until the neutron is absorbed or has been transmitted from the shell. On elastic collision, the neutron is scattered isotropically in the center-of-mass system, and for a heavy nucleus, such as gold, it is a reasonable simplification of the calculations if elastic scattering is taken to be isotropic in the laboratory system as well.

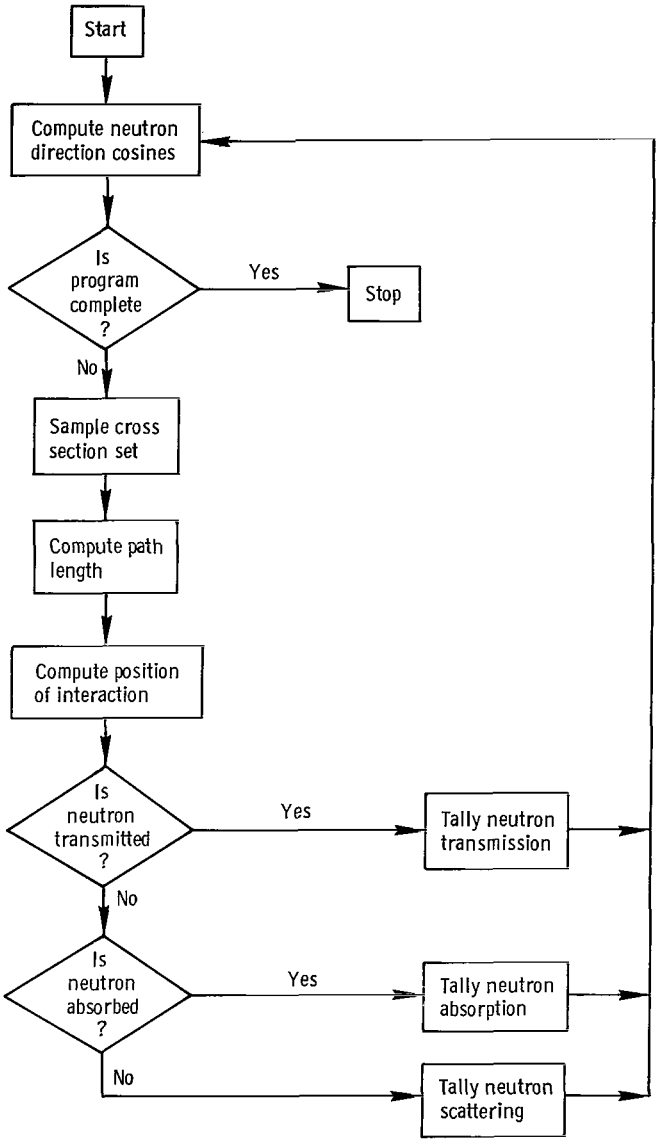

Figure 1. - Schematic description of Monte Carlo sphere transmission calculation.

A schematic description of the Monte Carlo sphere transmission calculation is shown in figure 1 and is further explained as follows:

(1) A cross section is chosen. (The generation of cross section is described in the next section.)

(2) A path length λ_r is chosen from an exponential distribution by the following equation:

$$\lambda_r = \frac{-\ln N_r}{\Sigma_t}$$

where N_r is a random number uniformly distributed on the open interval (0, 1) and Σ_t is the macroscopic total cross section.

(3) If λ_r terminates outside the shell, the neutron is tabulated as a transmission and a return is made to step 1.

(4) If λ_r terminates inside the spherical shell, the direction cosines of an isotropically emitted neutron are computed, and a new position of the neutron interaction is computed (ref. 15).

The cross sections are selected, and, if the collision is an absorption, the history is terminated. If the collision is a scattering, a return is made to step 1. The final output includes the transmission and the average cross sections for scattering and absorption.

STOCHASTIC CROSS SECTION GENERATION

The method of stochastic simulation is used to generate cross sections at 24 keV in order to accurately represent the behavior of the neutron trajectories in the spherical shell. This is done by applying the statistical distributions obtained from neutron resonance spectroscopy in the resolved energy region to neutron cross sections at 24 keV.

Desjardins et al. (ref. 16), in their measurements of the Au^{197} resonance parameters, were unable to assign J, the spin quantum number of the compound nucleus values to many of the resonances they resolved. Therefore only average values of the resonance parameters for the merged spin states were reported. The best-fit value of the merged s-wave strength function S_o was

$$S_o = \frac{\langle g\Gamma_n^o \rangle}{\overline{D}} = (1.5 \pm 0.3) \times 10^{-4}$$

where g is a statistical spin factor equal to $(2J + 1)/(4I + 2)$ and I is the spin quantum number of the nucleus investigated. The integral distribution of the reduced width neutron amplitudes Γ_n^o showed good agreement with a Porter-Thomas distribution. The merged spin average level spacing $\overline{D}$ was found to be 15.8 eV below 1000 eV, and 16.8 eV was suggested for the entire measured range to 1600 eV. However, when the integral distribution of gold-197 (Au^{197}) level spacings was compared with the distributions, for a random spacing of levels and with a single-species population Wigner distribution; the agreement is poor (ref. 17). Thus there was no agreement of the level spacing results of Desjardins et al. and these theoretical curves. Since gold has a nuclear spin $I = 3/2$,

the J = 1 levels are assumed to have a Wigner single-species population distribution, which is uncorrelated in position with respect to the J = 2 levels that are also assumed to be Wigner single-species population distribution. If the (2J + 1) spacing density applies, 3/8 of the levels should have J = 1 and the remaining 5/8 levels have J = 2. The Wigner two-species population curves, $D_1 = 5D_2/3$, gave good agreement when compared with the initial distribution; in fact, if $D_1 = D_2$ equally good fits can be obtained. The average parameters measured by Desjardins et al. of Columbia have been adjusted to 24 keV and are shown in table II.

TABLE II. - GOLD-197 STATISTICAL PARAMETERS USED IN CROSS SECTION GENERATOR

Source	Type of spins	Spin quantum number, I	Statistical spin factor, g	γ width, Γ_γ, meV	Neutron width, Γ_n, meV	Average level spacing, $\bar{D}$, eV
Ref. 16	Merged	1 and 2	0.500	170	780	16.8
Ref. 11	Merged	1 and 2	.500	125	930	15.5
	Separated	1	.375	125	930	44.0
		2	.625	125	930	24.0

More recently, Julien et al. (ref. 11) of Saclay have measured the spin-dependent statistical parameters of gold. Their results were different than those of Desjardins et al. The Saclay results were more in agreement with a value of $D_1 = 2.2\ D_2$. They found the reduced level width distribution functions as measured to agree with the theoretical Porter-Thomas distribution. They also found far better agreement between their results and the Wigner two-species population distribution than with a Wigner one-species population distribution. The average separated spin statistical parameters, as well as the merged values generated from the Saclay data, have been adjusted to 24 keV and are shown in table II.

With the statistical information obtained at low neutron energies, a series of "mock" or "pseudo" cross sections for the unresolved region are generated by the method of stochastic simulation. By making use of an adequate cross section set, as determined by the Central Limit Theorem, and a large energy spread for all resonances chosen ($E_0 \pm 100$ eV), a so-called resonance background is provided without the problem of the distribution of next nearest levels. The contribution of nearby resonances to the cross section is considered if the resonance is within 100 eV of the energy of the sampled cross section's energy. The use of a mock cross section set, decided on by these statistical

methods, ensures an average not subject to large fluctuations. Since both sets of s-wave capture cross sections are computed from independently chosen random number sequences, the uncorrelated aspect of the separate J-state resonances is assured.

Since calculation indicates that the peak values of the Doppler-broadened p-wave scattering resonances for Au^{197} at 24 keV are only of the order of a few tenths of a barn, the p-wave scattering is explicitly neglected, and any contribution to the total cross section by p-wave scattering is subsumed into the potential cross section.

In as much as both the Columbia and Saclay (refs. 7 and 8) data indicate that the distribution of the reduced scattering width amplitudes is Porter-Thomas, that is χ^2, the values for Γ_n have been chosen from a χ^2 distribution with one degree of freedom. The selection method is detailed in the appendix. Briefly, the values of $\overline{\Gamma}_n(J = 1)$ and $\overline{\Gamma}_n(J = 2)$ are computed for 24-keV neutrons. Next, the cumulative distribution function of $\Gamma_n(J = 1)/\overline{\Gamma}_n(J = 1)$ is divided into 10 intervals of equally probable values. The average value of $\Gamma_n/\overline{\Gamma}_n$ is found in each interval, and the corresponding value of Γ_n chosen. Thus, one is able to represent the Porter-Thomas distribution of $\Gamma_n/\overline{\Gamma}_n$ by a group of 10 equally probable Γ_n's per spin state.

The value of Γ_γ is assumed to be constant at 125 meV. It might be mentioned that 125 meV lies within the probable error range of 57 of the 63 resonances measured by the Saclay group between 0 and 1000 eV. This assumption, that of constant Γ_γ, is consistent with theory which indicates that Γ_γ should be distributed as χ^2 with a large number of degrees of freedom (ref. 18). Since the mean square deviation from the mean, for a normalized χ^2 distribution, is two over the number of degrees of freedom, Γ_γ should remain relatively constant from resonance to resonance (ref. 19).

A Doppler-broadening Breit-Wigner code is used to compute 10 or 20 resonance shapes, according to whether a merged spin-state or a separated spin-state cross section set is to be generated. The Doppler-broadening code computes values for the resonance cross sections from $(E_o - 100)$ to $(E_o + 100)$ eV by 0.5-eV increments, providing 401 energy dependent values of the cross sections per resonance. Figures 2 and 3 illustrate representative values of scattering and capture cross sections after Doppler-broadening for a merged spin-state calculation. The Wigner two-species level spacing distribution is chosen for the determination of the mock cross section's level spacings (ref. 17). The Wigner two-group distribution of level spacings shows the best agreement with the experimental data.

A single-group Wigner distribution is assumed for the merged spin calculations. This assumption is used to evaluate the error introduced into merged spin-state calculations. No correlation is introduced into the spin-dependent cross sections. Again, stratified sampling is used. The cumulative distribution function of the Wigner level spacing distribution is divided into 10 equally probable strata, and one shown in table III.

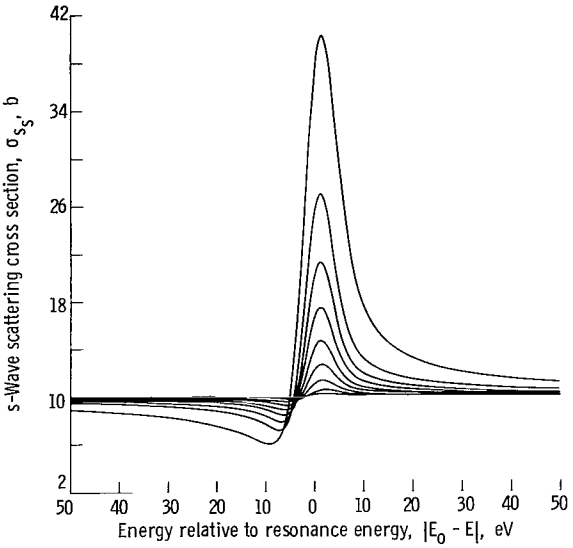

Figure 2. - Group s-wave scattering cross sections for gold. Potential cross section, 10 barns.

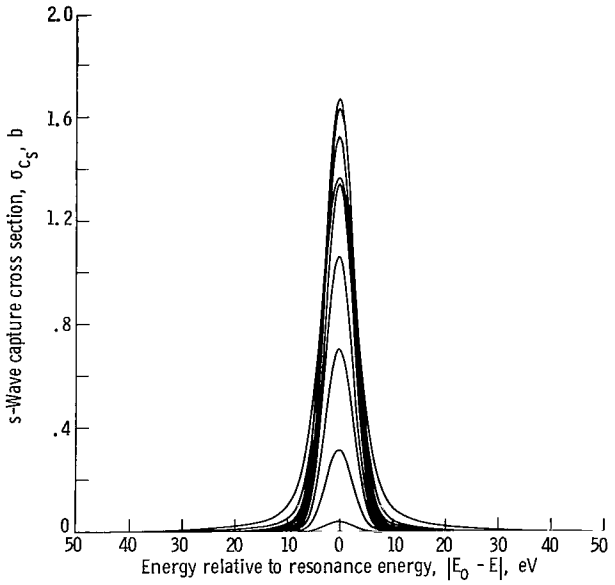

Figure 3. - Group s-wave capture cross sections for gold. Potential cross section, 10 barns.

TABLE III. - GROUP REPRESENTATION OF s-WAVE STATISTICAL DISTRIBUTIONS OF NEUTRON WIDTH AND LEVEL SPACING AT 24 keV FOR GOLD

Population range	Neutron width, $\Gamma_n(J = 1)$, meV	Neutron width, $\Gamma_n(J = 2)$, meV	Level spacing, $D_J(J = 1)$, eV	Level spacing, $D_J(J = 2)$, eV
0 to 1.0	930	930	44.0	24.0
0 to 0.1	9.3	9.3	11.5	6.5
0.1 to 0.2	40.5	40.5	20.0	11.0
0.2 to 0.3	102.3	102.3	26.0	14.0
0.3 to 0.4	226.5	226.5	31.0	17.0
0.4 to 0.5	339.0	339.0	38.0	20.5
0.5 to 0.6	539.9	539.9	43.0	23.5
0.6 to 0.7	827.7	827.7	49.0	27.0
0.7 to 0.8	1246.2	1246.2	58.0	31.5
0.8 to 0.9	1925.1	1925.1	68.0	37.0
0.9 to 1.0	4043.5	4043.5	95.5	52.0

These input data are useful for the stochastic generation of the spin-dependent cross sections. The procedure used to generate the cross sections in the unresolved energy region follows:

(1) A random integer, uniformly distributed in the interval 1 to 10, is chosen.

(2) One of the 10 resonances of a spin-state family, which corresponds to that random integer sampled in step 1, is chosen.

(3) A random integer, uniformly distributed in the interval 1 to 10, is chosen.

(4) Associated with the random integer just chosen is a level spacing, which is used to orient the next resonance obtained.

(5) Steps 1 to 4 are repeated until the cross sections associated with 10^6 energy points have been generated. The same procedure is repeated for the other spin state with a new random number sequence to ensure stochastic independence.

A question is posed as to how many of simulated cross sections generated, are necessary to represent adequately the entire set of one million cross sections. The question is answered in the following manner. The one million cross sections, for a single spin state, are divided into 2000 groups of 500 cross sections each, as well as, other various sized groupings. The mean value of each group is computed and the distribution of these mean values are plotted. It was found that the distribution of the mean values for groups of 10 000 assumes normality. Thus, by the Central Limit Theorem (refs. 20 and 21) a group of 10 000 is an adequate sample size for stochastic independence. The best set of 10 000 is chosen by matching the moments of the entire sample universe to each set of 10 000. The set whose first four moments best match the first four moments of the 10^6 cross sections is chosen as the most representative cross section set, for its particular spin state. This process is repeated for the other spin state.

The procedure has generated sets of cross sections that are compatible with the low-energy neutron spectrographic data and the assumed statistical distributions associated with the levels and their spacings. A stochastically simulated total cross section set for gold is shown in figure 4. It is clear that, although the average total cross section is 13.67 barns, local values at 24 keV vary from 6 to 40 barns.

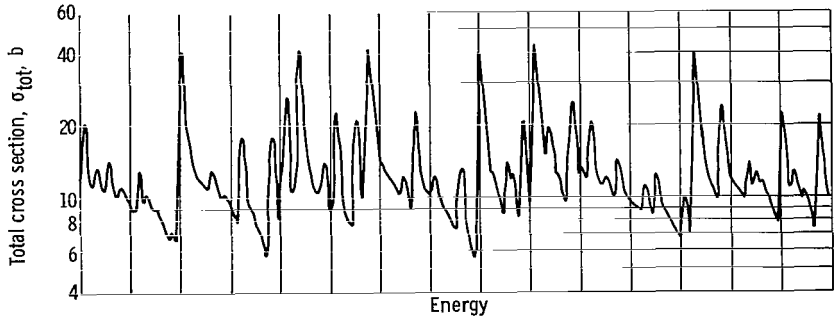

Figure 4. - Representative sample of generated set of total cross sections.

MONTE CARLO ANALYSIS OF GOLD SHELLS

The Monte Carlo transmission code described and the stochastically generated mock cross sections together with parametric values of both the potential cross section and the p-wave capture cross section are used to calculate values of transmission for 24-keV neutrons. Values of the neutron transmission are computed for the various gold spheres of Schmitt and Cook (ref. 7) as well as for the gold sphere of Belanova et al. (ref. 8).

The p-wave capture cross section is treated as an additive constant to the stochastically generated s-wave cross section sets because of the absence of measured p-wave statistics. Since there are four uncorrelated J-states for the p-wave resonances and if the Porter-Thomas distribution for p-wave resonances applies, it is a χ^2 distribution with two degrees of freedom. This distribution is not as widely a varying function as the χ^2 with one degree of freedom (ref. 19), and does not emphasize the many small values of $\Gamma_n/\overline{\Gamma}_n$ as the χ^2 with one degree of freedom does. Thus the assumption of a constant p-wave capture cross section seems reasonable.

With each value of potential cross section chosen, a new stochastic set of cross sections is generated and values of 6.00, 8.00, and 10.00 barns are used as the potential cross section for gold. The potential cross section σ_{pot} is chosen as a parameter to conserve the independently measured value of the total cross section σ_{tot} for gold of 13.67 barns. For a given value of σ_{pot}, several values of the average p-wave capture cross section $\overline{\sigma_{c_p}}$ are introduced and values of the neutron transmission are computed for each experimental shell. For each value of σ_{pot} a value of $\overline{\sigma_{c_p}}$ is found which is compatible with the experimentally measured value of transmission. Figure 5 illustrates

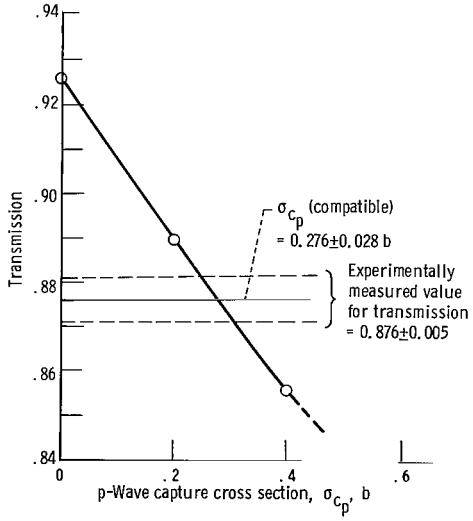

Figure 5. - Determination of p-wave capture cross section compatible with experimentally measured transmission for Au I sphere. Potential cross section, 6 barns.

TABLE IV. - TRANSMISSION COMPATIBLE VALUES

OF CROSS SECTIONS FOR Au I GOLD SPHERE[a]

Potential, σ_{pot}	s-Wave capture, $\overline{\sigma_{c_s}}$	s-Wave scattering, $\overline{\sigma_{s_s}}$	p-Wave capture, $\overline{\sigma_{c_p}}$	Total, $\overline{\sigma_{tot}}$
Cross section, b				
6.00	0.499	5.151	0.276	11.926
8.00	.499	5.147	.205	13.851
10.00	.499	5.150	.141	15.790

[a]Data from Schmitt and Cook (ref. 7).
[b]See fig. 5.

how the values of $\overline{\sigma_{c_p}}$ are obtained for the Au I sphere of Schmitt and Cook (ref. 7) for a σ_{pot} of 6.00 barns. This procedure is repeated for several values of σ_{pot}. Table IV indicates the calculated values of cross sections that are compatible with the experimental transmission for the Au I sphere for assumed values of the potential cross section. However, it is noted that the average total cross section $\overline{\sigma_{tot}}$ in the last column varies. Since $\overline{\sigma_{tot}}$ is measured independently, the results in table IV can be interpolated for best values of σ_{pot}, which is the only free cross section. In figure 6, a plot of $\overline{\sigma_{tot}}$ against σ_{pot} is shown. For this sphere transmission experiment, the potential and average

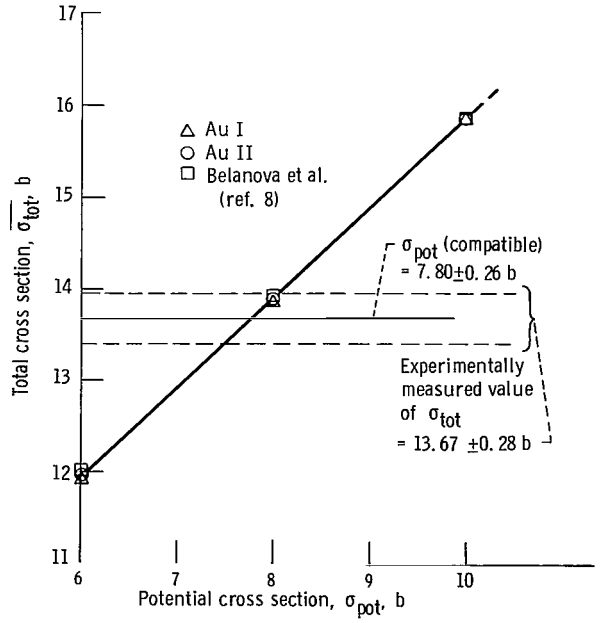

Figure 6. - Determination of potential cross section compatible with experimentally measured value of total cross section.

p-wave capture cross sections that best match the measured value of the total cross section have been obtained as $\sigma_{pot} = 7.80$ barns and $\overline{\sigma_{c_p}} = 0.226$ barn, respectively.

RESULTS AND CONCLUSIONS

The Monte Carlo cross section generation process permits accurate compilation of the statistical aspects of neutron cross sections and their associated distribution functions. The Monte Carlo transmission code permits analysis of average values of transmission by neutron trajectories in the spherical shell experiments.

Average Capture Cross Section

A Monte Carlo analysis for the merged spin statistics gives significantly different results than a similar analysis using separated spin states. The results of such analyses are shown in table V for the Schmitt and Cook (ref. 7) spheres. For the merged results,

TABLE V. - RESULTS OF GOLD SPHERE TRANSMISSION

ANALYSES BY MONTE CARLO

[[a]Total cross section for all cases, 13.7±0.3 b.]

Type of analysis	Cross section, b			
	s-Wave capture, $\overline{\sigma_{c_s}}$	s-Wave scattering, $\overline{\sigma_{s_s}}$	p-Wave capture, $\overline{\sigma_{c_p}}$	Potential, σ_{pot}
Unmerged[b]	0.499±0.012	5.15±0.12	0.226±0.025	7.8±0.3
Merged[b]	.465±0.010	4.45±0.10	.194±0.026	8.5±0.3
Merged[c]	.485±0.050	3.18±0.40	.150±0.015	9.9±0.4

[a]Value obtained from Duke University.
[b]Strength functions from ref. 11.
[c]Strength function from ref. 16.

both the Columbia unseparated statistics and the merged Saclay data, are used to obtain average cross sections. For gold there is an increase of about 35 millibarns of unmerged over the merged results for the s-wave capture. This may be expected because the merged spin state uses a single-species Wigner distribution and forces level repulsion.

The separated spin-state analysis on the other hand, forces level repulsion only within a particular spin state, allowing the uncorrelated separate spin states to aline without introducing a spin-spin level repulsion. The average s-wave scattering cross section is likewise increased for the same reason. The value of the potential cross section is lower for unmerged spins due to the increased value of the average s-wave scattering cross section. The reason for the larger value of the average p-wave capture cross section, for the separate spin-state analysis, appears to be that, since the value of the potential cross section is lower, more capture is necessary to maintain the correct value of the transmission coefficient.

TABLE VI. - AVERAGE CROSS SECTIONS FOR GOLD AT 24 keV

Experiment	Type of analysis	Shell dimensions, cm		Monte Carlo results					Transmission, b
		Outside radius	Inside radius	s-Wave scattering cross section, $\overline{\sigma_{s_s}}$, b	s-Wave capture cross section, $\overline{\sigma_{c_s}}$, b	p-Wave capture cross section, $\overline{\sigma_{c_p}}$, b	Capture cross section, $\overline{\sigma_c}$, b	Potential cross section, σ_{pot}, b	
[a]Au I	Merged	7.62	5.93	4.45±0.10	0.465±0.010	0.185±0.025	0.650±0.030	8.56±0.31	0.876±0.005
	Unmerged	7.62	5.93	5.15±0.12	.499±0.012	.211±0.026	.710±0.031	7.80±0.28	.876±0.005
[a]Au II	Merged	7.62	5.08	4.45±0.10	0.465±0.010	0.204±0.028	0.669±0.032	8.54±0.30	0.800±0.004
	Unmerged	7.62	5.08	5.14±0.12	.499±0.012	.238±0.029	.737±0.033	7.78±0.28	.800±0.004
[b]Long counter	Merged	3.55	2.05	4.45±0.10	0.465±0.010	0.259±0.023	0.724±0.029	8.49±0.30	0.895±0.002
	Unmerged	3.55	2.05	5.15±0.12	.499±0.012	.275±0.025	.774±0.031	7.74±0.28	.985±0.002

[a]Ref. 7.
[b]Ref. 8.

The final results are shown in table VI which compares the results of a merged Saclay statistics Monte Carlo analysis for the individual spheres with results for the separated Saclay statistics giving the individual cross sections derived from each sphere transmission experiment. The average unmerged value of $\overline{\sigma_c}$ for the Schmitt and Cook (ref. 7) experiments is 725±30 millibarns. The corresponding merged value of $\overline{\sigma_c}$ is 660±30 millibarns. The average unmerged value of $\overline{\sigma_c}$ for the Schmitt and Cook experiments is likewise in good agreement with the recent gold activation measurement of Harris et al. (ref. 5) of 713±40 millibarns. The average unmerged value of $\overline{\sigma_c}$ for Belanova et al. (ref. 8) is 774±31 millibarns and likewise the merged value is 724±29 millibarns.

Average Potential Cross Section

The results of the Monte Carlo analysis for gold indicate a potential cross section of

7.80±0.28 barns. This disagrees with a measured low-energy value of σ_{pot} (11.2 b, ref. 22) obtained by subtracting resonance contributions to the total cross section in the resolved region. The present result of 7.80 barns at 24 keV may be converted to its low-energy value by a partial wave analysis using the rigid-sphere model (ref. 22) to provide a value of 8.00 barns. With this model, the difference between σ_{pot} at 24 keV and at low energy is small (2.5 percent). Since σ_{pot} is given by $4\pi(R')^2$, the radius implied by the potential cross section of 7.80 barns is 7.88×10^{-13} centimeter. This result is in remarkable agreement with the value of 7.86×10^{-13} centimeter obtained from the strong interaction model $R' = R = 1.35\times A^{1/3}$ centimeter, where R' is the potential scattering radius and R is the nuclear radius. The discrepancy between the measured (ref. 22) $\sigma_{pot} = 11.2$ barns and the smaller Monte Carlo result may be due to an underestimation of the scattering cross section due to nearby low-energy resonances in reference 22. The value of R' as given by the Monte Carlo analysis is compared with the average radial density distribution for the Au^{197} nucleus as determined by electron scattering (ref. 24) in figure 7. The normalized density $\rho(r)/\rho(0)$ is 0.05 at a radius of 7.80×10^{-13} centimeter and is virtually zero at 8.00×10^{-13} centimeter. Therefore, there is good agreement between the Monte Carlo estimate for the nuclear radius and the nuclear density distribution as ascertained by electron scattering experiments, whereas the value of R reported by Seth et al. (ref. 22) is considerably larger.

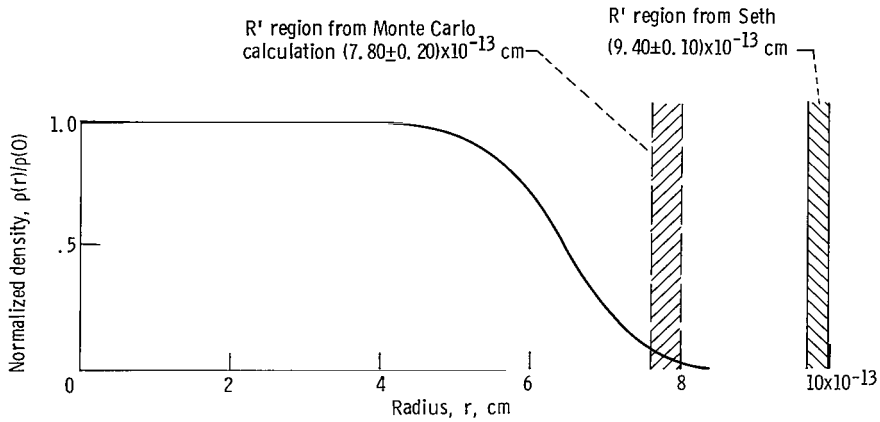

Figure 7. - Normalized radial density distribution compared with Monte Carlo potential scattering radius R' and R' of Seth et al. (ref. 23).

The total average scattering cross section $\overline{\sigma_s}$ as determined by Monte Carlo is 12.95±0.20 barns as compared with the measurement of Langsdorf et al. (see ref. 25) of 12.80±0.20 barns; this indicates good agreement between the present Monte Carlo analysis and an independently measured value of $\overline{\sigma_s}$.

It may be recalled that the only free parameters in the present analysis are the potential cross section and the average p-wave capture cross section. They are adjusted to fit the total cross section and the transmission, respectively. Thus the agreement of the potential cross section with the other independently measured and computed quantities and the agreement of the Monte Carlo total average scattering cross section with that of Langsdorf are additional contributory evidence for the validity of the Monte Carlo results.

A method for the generation of cross sections in the unresolved energy region has been illustrated and used to evaluate and interpret Au^{197} spherical shell neutron transmission experiments.

Lewis Research Center,
National Aeronautics and Space Administration,
Cleveland, Ohio, February 20, 1969,
129-02-04-04-22.

APPENDIX - METHOD OF STRATIFIED SAMPLING

The production of the generated cross sections in the unresolved region entails the sampling from two probability distributions, the Wigner line spacing distribution and the Porter-Thomas distribution of neutron widths. Since both distributions are known and may be expressed analytically, one might be tempted to sample in a direct manner from both these distributions. One could continuously map the uniformly distributed random number generator on the two cumulative probability distributions and for each sampling of a random number in the interval (0, 1) obtain through the mapping, a value of the sampled variable (ref. 26). However, this process has been rejected for reasons which shall now be illustrated. The Wigner line spacing distribution may be written as

$$P\left(\frac{D}{\langle D\rangle}\right) = \frac{\pi D}{2\langle D\rangle^2} \exp\left(\frac{-\pi D^2}{4\langle D\rangle^2}\right)$$

If one makes the simple transformation, $x = D/\langle D\rangle$ one obtains

$$P(x) = \frac{\pi}{2} \frac{x}{\langle D\rangle} \exp\left(-\frac{\pi}{4} x^2\right)$$

If one then forms the functional mapping

$$R_n = \int_0^X \frac{\pi}{2} x \exp\left(-\frac{\pi}{4} x^2\right) dx$$

and solves for X, one finds

$$X = \frac{2}{\sqrt{\pi}} \sqrt{-\ln(1 - R_n)}$$

Thus, to choose from the Wigner level spacing distribution in a continuous manner, first a random number must be chosen in the interval (0, 1), then that number subtracted from 1. Next the natural logarithm of the difference is taken, the sign of the natural logarithm is changed, the square root of the logarithm is taken, and that result is then multiplied by $2/\sqrt{\pi}$. Thus in the production of one random sample from the Wigner distribution at least one subtraction, one multiplication, and three function evaluations are performed. Hence, for an IBM 7094-II, the time necessary for one sampling is of the order of 450 microseconds, a similar calculation for the Porter-Thomas distribution

gives much larger generation times. In order to reduce the amount of time required to generate cross sections and to reduce the variance associated with such a generated set, the technique of stratified sampling is used.

Stratified sampling consists of dividing the population to be sampled into various strata with appropriate weighting and then the choosing values from each stratum to represent the distribution within that stratum (ref. 27). In this particular application, the cumulative probability distribution functions of both the Wigner and Porter-Thomas distribution are divided into 10 equally probable strata. Then the average value within each stratum is obtained. These values are chosen to preserve the average value of the entire distribution. The values, thus obtained, are checked using the Kolmogorov-Smirnov test for goodness of fit (ref. 28) and other statistical methods. Both the Porter-Thomas and the Wigner samples are accepted at the 99-percent level of the Kolmogorov-Smirnov test. A comparison of the moments of stratified samples and some random samples is shown in table VII. This comparison indicates the power of the stratified

TABLE VII. - WIGNER LEVEL SPACING

Sample size	Moments about mean				
	μ_1	μ_2	μ_3	μ_4	μ_2
Stratified sample					
10	0	0.3209	0.1420	0.3403	0.3265
∞	0	.2732	.0901	.2423	.2341
Random sample					
40	0.0486	0.3516	0.2266	0.5030	0.7557
100	.0189	.2972	.1154	.2873	.3207
500	.0462	.2846	.1409	.3053	.3981
1000	0.	.2732	.0901	.2422	.2341

sampling technique, in that the stratified sample size of 10 gives an approximation of the exact moments which is matched only after sampling randomly hundreds of values. The same is true for the Porter-Thomas distribution.

REFERENCES

1. Cox, S. A.: Fast Neutron Cross Sections: keV to MeV. Proceedings of the Second Conference on Neutron Cross Sections and Technology, Washington, D.C., Mar. 4-7, 1968. Spec. Publ. 299, National Bureau of Standards Vol. 2, Sept. 1968, pp. 701-727.

2. Poenitz, W. P.: An Absolute (n,γ)-Cross Section Measurement for Gold at 30 keV and Its Application in Normalization of Other Data. IAEA Conference Proceedings Paris, Nuclear Data for Reactors, Vol. 1, Oct. 17-21, 1966, pp. 277-294.

3. Bogart, Donald: Boron Cross Sections As A Source of Discrepancy for Capture Cross Sections in the keV Region. Neutron Cross Section Technology. AEC Rep. CONF-660303, Book 1, Mar. 24, 1966, pp. 486-501.

4. Poenitz, W. P.; Kompe, D.; and Menlove, H. O.: The Neutron Capture Cross Section of Gold in the keV Energy Region. J. Nucl. Energy, vol. 22, no. 8, Aug. 1968, pp. 505-515.

5. Ryves, T. B.; Robertson, J. C.; Axton, E. J.; Goodier, I.; and Williams, A.: The Radiative Capture Cross Section of Gold at the Energy of Sb-Be Photoneutrons. J. Nucl. Energy, Pts. A/B, vol. 20, 1966, pp. 249-260.

6. Harris, K. K.; Grench, H. A.; Johnson, R. G.; Vaughn, F. J.; Ferziger, J. H.; and Sher, R.: The Au^{197} (n,γ) Au^{198} Cross Section from 13 keV to 683 keV. Nucl. Phys., vol. 69, 1965, pp. 37-48.

7. Schmitt, H. W.; and Cook, C. W.: Absolute Neutron Absorption Cross Sections for Sb-Be Photoneutrons. Nucl. Phys., vol. 20, 1960, pp. 202-219.

8. Belanova, T. S.; Van'kov, A. A.; Mikhailus, F. F.; and Stravisskii, Yu. Ya.: Absolute Measurements of the Absorption Cross Sections of 24 keV Neutrons. J. Nucl. Energy, Pts. A/B, vol. 20, 1966, pp. 411-417.

9. Bogart, Donald; and Semler, Thor T.: Monte Carlo Interpretation of Sphere Transmission Experiments for Average Capture Cross Sections at 24 keV. Neutron Cross Section Technology. AEC Rep. CONF-660303, Book 1, Mar. 24, 1966, pp. 502-521.

10. Bogart, Donald: An Improved Analysis of Sphere Transmission Experiments for Average Capture Cross Sections. IAEA Conference Proceedings Paris, Nuclear Data for Reactors, Vol. I, Oct. 17-21, 1966, pp. 503-511.

11. Julien, J.; DeBarros, S.; Bianchi, G.; Corge, C.; Huynh, V. D.; LePoittevin, G.; Morgenstern, J.; Netter, F.; Samour, C.; and Vastel, R.: Détermination Du Spin Et Des Paramètres Des Résonances Pour ^{197}Au + n de 10 eV a 1000 eV. Nucl. Phys., vol. 76, 1966, pp. 391-432.

12. Bethe, H. A.; Beyster, J. R.; and Carter, R. E.: Inelastic Cross-Sections for Fission-Spectrum Neutrons-I. J. Nucl. Energy, vol. 3, no. 3, pt. I, 1956, pp. 207-223.

13. Bethe, H. A.; Beyster, J. R.; and Carter, R. E.: Inelastic Cross Sections for Fission-Spectrum Neutrons-II. J Nucl. Energy, vol. 3, no. 4, pt. I, 1956, pp. 273-300.

14. Bethe, H. A.; Beyster, J. R.; and Carter, R. E : Inelastic Cross-Sections for Fission-Spectrum Neutrons-III. J. Nucl. Energy, vol. 4, no. 1, pt. I, 1957, pp. 3-25.

15. Clark, Melville, Jr.; and Hansen, Kent F.: Numerical Methods of Reactor Analysis. Academic Press, 1964.

16. Desjardins, J. S.; Rosen, J. L.; Havens, W. W., Jr.; and Rainwater, J.: Slow Neutron Resonance Spectroscopy. II. Ag, Au, Ta. Phys. Rev., vol. 120, no. 6, Dec. 15, 1960, pp. 2214-2226.

17. Wigner, E. P.: Results and Theory of Resonance Absorption. Conference on Neutron Physics by Time-of-Flight, Gatlinburg, Tenn., Nov. 1-2, 1956. Rep. ORNL-2309, Oak Ridge National Lab., 1957, pp. 59-70.

18. Porter, C. E.; and Thomas, R. G.: Fluctuations of Nuclear Reaction Widths. Phys. Rev., vol. 104, no. 2, Oct. 15, 1956, pp. 483-491.

19. Preston, Melvin A.: Physics of the Nucleus. Addison-Wesley Pub. Co., Inc., 1962, pp. 505-508.

20. Parzen, Emanuel: Modern Probability Theory and Its Applications. John Wiley & Sons, Inc., 1960.

21. Cramer, Harald: Mathematical Methods of Statistics. Seventh ed., Princeton University Press, 1957.

22. Seth, K. K., Huges, D. J.; Zimmerman, R. L.; and Garth, R. C.: Nuclear Radii by Scattering of Low-Energy Neutrons. Phys. Rev., vol. 110, no. 3, May 1, 1958, pp. 692-700.

23. Schiff, Leonard I.: Quantum Mechanics. Second ed., McGraw-Hill Book Co., Inc., 1955, pp. 110-111.

24. Elton, Lewis R. B.: Nuclear Sizes. Oxford University Press, 1961, pp. 27-36.

25. Goldberg, Murrey D.; Mughabghab, Said F.; Purohit, Surendra N.; Magurno, Benjamin A.; and May, Victoria M.: Neutron Cross Sections. Vol. IIC, Z = 61 to 87. Rep. BNL-325, 2nd ed., suppl. 2, vol. IIC, Brookhaven National Lab., Aug. 1966, p. 79-0-13.

26. Hammersley, J. M.; and Handscomb, D. C.: Monte Carlo Methods. John Wiley & Sons, Inc., 1964.

27. Kish, Leslie: Survey Sampling. John Wiley & Sons, Inc., 1965.

28. Lindgren, Bernard W.; and McElrath, G. W.: Introduction to Probability and Statistics. Macmillan Co., 1959, p. 261.

NASA-Langley, 1969 —— 24 E-4811

NATIONAL AERONAUTICS AND SPACE ADMINISTRATION
WASHINGTON, D. C. 20546

OFFICIAL BUSINESS

FIRST CLASS MAIL

POSTAGE AND FEES PAID
NATIONAL AERONAUTICS AND
SPACE ADMINISTRATION

POSTMASTER: If Undeliverable (Section 158 Postal Manual) Do Not Return

"The aeronautical and space activities of the United States shall be conducted so as to contribute . . . to the expansion of human knowledge of phenomena in the atmosphere and space. The Administration shall provide for the widest practicable and appropriate dissemination of information concerning its activities and the results thereof."

—NATIONAL AERONAUTICS AND SPACE ACT OF 1958

NASA SCIENTIFIC AND TECHNICAL PUBLICATIONS

TECHNICAL REPORTS: Scientific and technical information considered important, complete, and a lasting contribution to existing knowledge.

TECHNICAL NOTES: Information less broad in scope but nevertheless of importance as a contribution to existing knowledge.

TECHNICAL MEMORANDUMS: Information receiving limited distribution because of preliminary data, security classification, or other reasons.

CONTRACTOR REPORTS: Scientific and technical information generated under a NASA contract or grant and considered an important contribution to existing knowledge.

TECHNICAL TRANSLATIONS: Information published in a foreign language considered to merit NASA distribution in English.

SPECIAL PUBLICATIONS: Information derived from or of value to NASA activities. Publications include conference proceedings, monographs, data compilations, handbooks, sourcebooks, and special bibliographies.

TECHNOLOGY UTILIZATION PUBLICATIONS: Information on technology used by NASA that may be of particular interest in commercial and other non-aerospace applications. Publications include Tech Briefs, Technology Utilization Reports and Notes, and Technology Surveys.

Details on the availability of these publications may be obtained from:

SCIENTIFIC AND TECHNICAL INFORMATION DIVISION

NATIONAL AERONAUTICS AND SPACE ADMINISTRATION

Washington, D.C. 20546